Facile Fabrication of Renewable Wood-Derived Carbon/SiBCN Aerogel Composites for High-Performance Microwave Absorption

Yuan Ke[#], Shangbo Han[#], Lingyu Yang, Xianqi Chen, Peitao Hu, Changqing Hong and Shun Dong[*]

Science and Technology on Advanced Composite in Special Environments Laboratory, Harbin Institute of Technology, Harbin 150001, China

Abstract: With the rapid development of communication technologies, there is an urgent demand for high-performance microwave absorbing materials. Wood-derived carbon (WDC), characterized by its lightweight, renewable, low-cost, and tunable dielectric properties, is regarded as a core candidate for future green microwave absorbing materials. However, pure WDC exhibits relatively limited microwave absorption performance. Thus, this work demonstrates a facile strategy for integrating WDC with SiBCN aerogels via controlled growth within the WDC matrix, achieved through a two-step sol-gel process combined with thermal treatment. SiBCN aerogel particles formed a typical three-dimensional network structure within the pores of WDC. The resulting WDC/SiBCN aerogel composite achieved a minimum reflection loss (RL_{min}) of -46.0 dB at a thickness of only 1.71 mm, with an effective absorption bandwidth (EAB) of 3.60 GHz, which demonstrates significantly enhanced microwave absorption performance compared to existing similar systems. The performance improvement is attributed to the synergistic effects of dipole polarization, multiple reflection mechanisms, and excellent impedance matching between the SiBCN aerogel and wood-derived carbon. This research provides a novel strategy for fabricating WDC/SiBCN aerogel composites that combine renewability with superior microwave absorbing capabilities.

Keywords: Composite, Microwave absorption, Reflection loss, Sol-gel and thermal treatment method, SiBCN aerogel, Wood-derived carbon.

1. INTRODUCTION

In recent years, with the rapid popularization of 5G technology, the virtual reality and smart home industries have flourished, and the quality of human life has been significantly improved. However, behind the rapid development of communication technology, the problems brought by microwaves have become increasingly prominent. It not only causes serious pollution to the environment, interferes with the normal operation of advanced electronic devices, but also poses a threat to public health. Consequently, developing renewable materials with superior microwave absorption capabilities has become a paramount research objective [1-4].

Wood-derived carbon (WDC), obtained by pyrolyzing renewable wood, serves as a sustainable, lightweight, and hierarchically porous building block for green composite microwave absorbers, where its bio-based origin and scalable processing align well with the emerging development of environmentally friendly wood-based absorbing/shielding composites [5], owing to its unique dielectric properties, excellent structural tunability, and environmentally friendly characteristics in recent years [6, 7]. However, the microwave absorption performance of WDC is usually not outstanding, because their high conductivity leading to poor impedance matching [8]. For example, Qin *et al*. [2] have tested the microwave absorption performance of WDC whose minimum reflection loss >-10dB. Therefore, many studies have been conducted to enhance the microwave absorption performance of wood. Dong *et al*. [9] investigated that the RL values of porous biomass-derived carbon (PBDC) prepared from teak wood all exceeded -10 dB, indicating its limited microwave absorption performance. By introducing manganese dioxide (MnO_2) nanowires into the PBDC matrix through a facile method, the resulting three-dimensional MnO_2 nanowires/PBDC composite exhibited optimized impedance matching and enhanced microwave absorption properties. When the thickness was 2.47 mm, the RL_{min} reached -51.6 dB at 10.4 GHz, with an effective absorption bandwidth (EAB) of 4.7 GHz, demonstrating significantly improved microwave absorption performance compared to the pristine PBDC material. Lou *et al*. [10] demonstrated that natural wood shavings exhibit ineffective microwave absorption performance. However, by subjecting pre-prepared Fe_3O_4/wood chip composites to in-situ carbonization at 1000 °C, they successfully synthesized porous carbon matrix with inlaid Fe_3C/Fe_3O_4 micro-particles (CFF). This composite achieved an optimal RL_{min} of -26.72 dB at a thickness of 3.15 mm. Thus, the strategy of compositing WDC with other wave-absorbing materials have already been proved to be a practicable method to improve the

*Address correspondence to this author at the School of Aeronautics, Harbin Institute of Technology, No.2 YiKuang Street, Harbin, Science Park of HIT Heilongjiang Province, PR China, 150001; Tel: +86-451-8641-2114; E-mail: dongshun@hit.edu.cn

[#]Yuan Ke and Shangbo Han contributed equally to this work.

Received on 14-11-2025 Accepted on 22-12-2025 Published on 29-12-2025

E-ISSN: 2311-8717/25

microwave absorption performance of pure WDC and also has garnered significant attention from researchers. Apart from these conventional magnetic-loss microwave absorbers, which probably tend to degrade or fail under high-temperature conditions, dielectric absorbers represent another major class of candidates that can likewise be leveraged to improve the microwave absorption performance of wood-derived carbon [11]. Among these, precursor-derived silicon-based ceramics are usually considered excellent materials for modification due to their high-temperature resistance, superior dielectric properties, and easy compositional tenability [12]. In particular, SiBCN [13], compared to other precursor-derived silicon-based ceramics such as SiOC [14] and SiCN [15], exhibits superior thermal stability.

Extensive research has been conducted on the microwave absorption properties of SiBCN and its composites, yielding significant advances. Zhang *et al*. [16] prepared SiBCN ceramic aerogels via a combination of freeze-drying and polymer-derived ceramics (PDCs) methods, using polyborosilazane (PBSZ) and divinylbenzene as precursors and crosslinking agents, respectively, through hydrosilylation reaction. The SiBCN ceramic aerogel samples achieved a RL_{min} of -25.05 dB and an EAB of 5.75 GHz at a thickness of 3 mm. This indicates that SiBCN inherently possesses great microwave absorption performance. Jiang *et al*. [17] conducted a study on the microwave absorption performance of C/SiC/SiBCN composites and found that combining C/SiC with SiBCN aerogels results in excellent microwave absorption performance, achieving a RL_{min} of -45.7 dB with an effective bandwidth of 5.3 GHz. Collectively, the aforementioned research findings suggest that incorporating SiBCN ceramic aerogels with dielectric loss materials could further improve and tailor the microwave absorption properties of the resulting composites. From a composite-design perspective, WDC is employed as a renewable, anisotropic, and hierarchically porous scaffold, while SiBCN aerogel serves as a lightweight dielectric phase grown in situ to construct a multiscale hybrid architecture. Accordingly, the PBSZ concentration is used as a practical design knob to tune SiBCN loading, connectivity, and potential percolation-like network formation within the WDC framework. Following this approach, integrating SiBCN ceramic aerogels with WDC could leverage the advantages of both of their unique porous architectures and holds the potential to yield a composite with excellent microwave absorption performance. However, current studies in this area remain limited.

Here, we prepared WDC/SiBCN aerogel composites by a two-step sol-gel and heat-treatment method. The experimental findings indicate that WDC/SiBCN aerogel composites exhibited superior microwave absorption performance compared to WDC. The synthesized WDC/SiBCN aerogel composite possesses both the unique porous structure of WDC and the network structure formed by SiBCN aerogel particles. When the SiBCN content is 5% and the material thickness is 1.71 mm, RL_{min} reaches -46.0 dB, with an EAB of 3.60 GHz. Excellent microwave absorption performance of the WDC/SiBCN aerogel composites indicates broad application prospects in the field of renewable materials and electromagnetic pollution protection.

2. MATERIALS AND METHODS

2.1. Raw Materials

PBSZ, serving as the precursor for SiBCN aerogel, was obtained from the Institute of Chemistry, Chinese Academy of Sciences. Divinylbenzene (DVB), supplied by Macklin in China, was used as a crosslinking agent. Cyclohexane and ethanol were purchased from Tianjin Kemiou Chemical Co. Ltd., China. All reagents and solvents were utilized without any further treatment.

2.2. Preparation of WDC/SiBCN Aerogel Composites

The raw wood block was placed in an argon atmosphere and heated at a rate of 3 °C/min to 1200 °C for 1 hour to obtain WDC. PBSZ and DVB were added to cyclohexane (in a mass ratio of 1:1), and solutions with precursor concentrations of 5wt.%, 10wt.%, and 15wt.% were thoroughly stirred at room temperature for 10 minutes to obtain homogeneous solutions. The three samples were designated as WDC/SiBCN-5, WDC/SiBCN-10, and WDC/SiBCN-15, respectively. The samples that did not undergo any further processing were named WDC. Then, WDC was immersed in the above solutions and placed in a beaker for thorough soaking. Subsequently, a solvothermal treatment was conducted at 120 ℃ for 20 hours to obtain the WDC/SiBCN wet gel composite material. Subsequently, the composite material was soaked in ethanol for 5 days for solvent replacement, with the anhydrous ethanol being changed every 12 hours. Then, it was dried to obtain the WDC/SiBCN dry gel composites. Finally, the composite was placed in an argon atmosphere and heated at 1000 ℃ at a heating rate of 3 ℃/min for 2 hours to obtain the WDC/SiBCN aerogel composites. The preparation process is illustrated schematically in Figure **1**. Besides that, SiBCN aerogels were also fabricated using the same process without adding WDC.

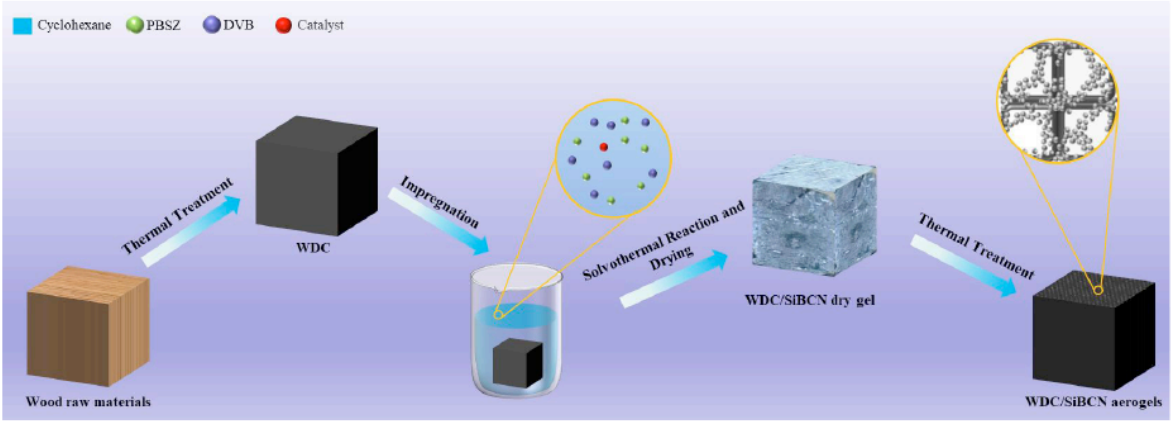

Figure 1: Preparation steps of WDC/SiBCN aerogel composites.

2.3. Characterization and Measurement

The crystal structure of WDC/SiBCN aerogel composites was systematically analyzed by using a German Bruker D8 ADVANCE X-ray diffractometer (XRD) with Cu K_α radiation ($\lambda = 1.54$ Å) as the radiation source. The morphology of the composites was characterized using field-emission scanning electron microscopy (SEM, S4800, Hitachi, Japan). The microwave absorption measurements involved the determination of the relative complex permittivity ($\varepsilon_r = \varepsilon' - j\varepsilon''$) and complex permeability ($\mu_r = \mu' - j\mu''$) using a Vector Network Analyzer (ZNA43, Rohde & Schwarz) across the frequency range of 2-18 GHz. Samples were prepared by blending the WDC/SiBCN aerogel composite with paraffin wax (constituting 70 wt.% of the mixture) at 90 °C. The resulting mixture was subsequently molded into hollow cylindrical shapes with an outer diameter of 7.00 mm and an inner diameter of 3.04 mm. The EMW absorption properties of the samples were evaluated based on their RL values, with the input impedance (Z_{in}) calculated using the following equations. (1) and (2) [18-22].

$$RL(dB) = 20\lg\left|\frac{Z_{in} - Z_0}{Z_{in} + Z_0}\right| \quad (1)$$

$$Z_{in} = Z_0\sqrt{\frac{\mu_r}{\varepsilon_r}}\tanh\left[j\frac{2\pi fd}{c}\sqrt{\mu_r\varepsilon_r}\right] \quad (2)$$

where Z_0, Z_{in}, f, d, and c denote the intrinsic impedance of free space, the input impedance of the absorber, the microwave frequency of the EMW, the thickness of the specimen, and the velocity of the EMW in free space, respectively.

3. RESULTS AND DISCUSSION

3.1. Characterization of WDC/SiBCN aerogel composites

Figure **2**(**a**) presents the X-ray diffraction patterns of WDC/SiBCN aerogel composites with different SiBCN aerogel content. In these patterns, apart from two broad peaks corresponding to the graphite peaks at about 26.3° and 43.0°, no sharp crystalline peaks were observed. This is attributed to the (002) and (101) crystal planes of the amorphous carbon phase [23]. The results confirm that WDC and SiBCN retain their amorphous structure even after pyrolysis at 1200 °C and 1000 °C.

In light of previous research, the graphitization degree of carbon - based composites significantly influences their microwave absorption performance [24, 25]. To delve deeper into the carbon nanostructure, Raman spectroscopy was further utilized to explore the *in situ* formation of sp^2 carbon within the aerogel [26]. The D band, located at 1350 cm^{-1}, represents the defects existing within the carbon atomic crystal lattice. It reflects the absence of a well - defined structure and the low orientation of free carbon. The G band, positioned at 1580 cm^{-1}, corresponds to the stretching vibration within the sp^2 - hybridized graphite plane of carbon atoms, which is associated with the graphitization degree of the aerogel [27]. The intensity ratio I_D/I_G of the D band and the G band serves as an indicator of the carbon's graphitization degree and the disorder of its defects [28]. A higher I_D/I_G ratio indicates lower graphitization degree and greater structural disorder. The Raman spectroscopy data were processed by curve fitting using Gaussian functions [29], where the I_D/I_G ratio was calculated based on the integrated area of the corresponding peaks [30]. As depicted in the Figure **2**(**b**), the I_D/I_G value of WDC/SiBCN-5 is 1.842, for WDC/SiBCN-10, it is 1.861; and for WDC/SiBCN-15, the I_D/I_G value is 1.836. The close agreement among these three values indicates comparable graphitization degrees between the samples, which is primarily attributed to their identical thermal treatment conditions. This also indicates that the all samples contain a high proportion of disordered carbon than sp^2-hybridized carbon, with low graphitization degree, consequently demonstrating

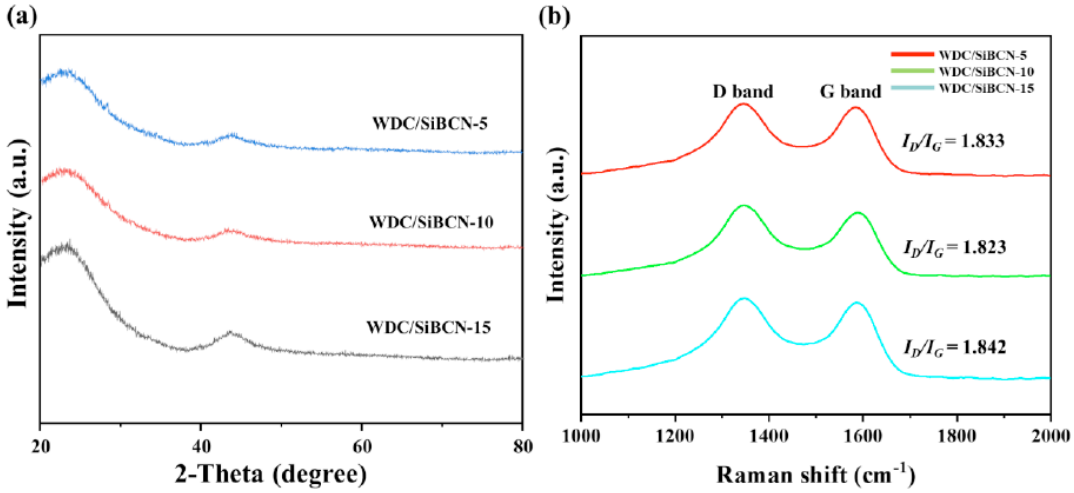

Figure 2: (**a**) XRD patterns of WDC/SiBCN aerogel composites; (**b**) Raman spectra of WDC/SiBCN aerogel composites.

high defect density. According to previous research, defects can act as polarization centers and dissipate more energy, leading to stronger absorption performance [31]. This implies that a higher defect content is beneficial for improving absorption performance. However, the number of defects is not the sole determinant of absorption properties [32], and other influencing factors will be analyzed in the following sections.

The morphologies and microstructures of WDC and WDC/SiBCN are shown in Figure **3**. Figure **3**(**a**) reveals the WDC framework after 1200 °C thermal treatment, exhibiting a regularly arranged porous architecture. Figure **3b** enables a more detailed observation of the details of the pore structure. It can be seen that the inner surface of the pores is uneven. This unique structure provides possible growth sites for SiBCN aerogel particles.

Figure **3c**-**h** present the microstructural characteristics of WDC/SiBCN aerogel composite. It can be clearly observed that the pristine WDC surface is relatively smooth and flat, showing no obvious particulate features. After introducing the SiBCN aerogel phase, numerous fine particles emerge and progressively decorate the WDC surface, confirming that SiBCN aerogel particles have successfully adhered to and grown on the carbon scaffold. Notably, as the PBSZ concentration is gradually increased, the introduced amount of SiBCN correspondingly rises, leading to a steady increase in the surface coverage and particle density on WDC. This evolution directly reshapes the composite architecture: at low PBSZ concentrations, the SiBCN phase appears mainly as sparsely distributed particles anchored on the WDC walls which form a nascent aerogel network; at intermediate concentrations, the particle population becomes denser and begins to form locally interconnected clusters; and at a PBSZ concentration of 15 wt%, a more continuous and clearly discernible three-dimensional, particle-assembled network develops across the WDC surface, partially spanning

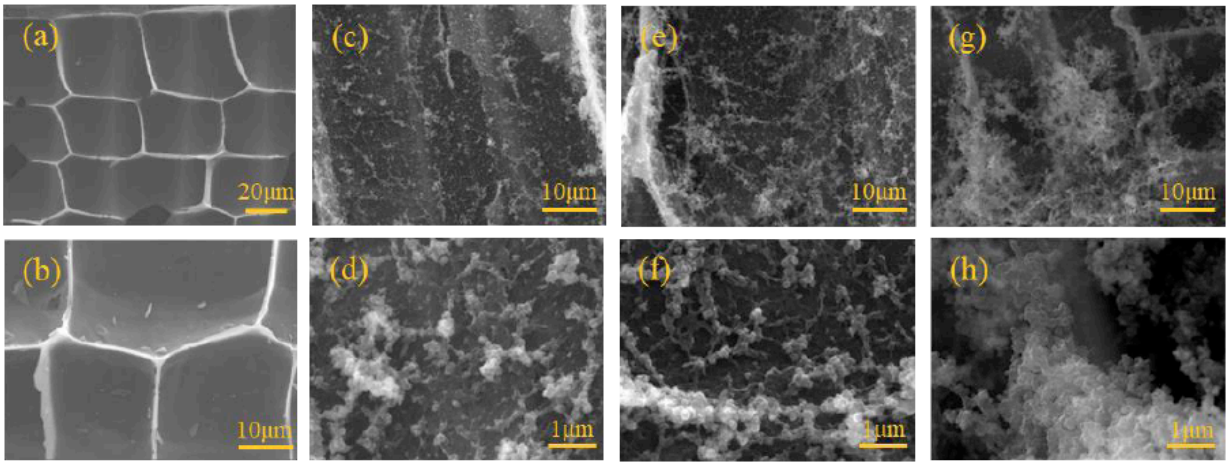

Figure 3: SEM images of WDC and WDC/SiBCN aerogel composites; (**a**, **b**) WDC; (**c**, **d**) WDC/SiBCN-5;(**e**, **f**) WDC/SiBCN-10;(g, h) WDC/SiBCN-15.

pore openings and bridging adjacent regions. Meanwhile, the agglomeration of SiBCN aerogel particles becomes increasingly prominent with increasing PBSZ concentration, and inter-agglomerate connections composed of SiBCN particles gradually form between neighboring agglomerates, giving rise to a hierarchical architecture. Overall, varying the SiBCN loading drives a transition from a smooth WDC surface to a particulate-decorated surface and ultimately to an interconnected 3D SiBCN network, thereby providing a tunable composite microstructure for subsequent structure–property correlations.

More specifically, some SiBCN particles in the images Figure **3d** and f exhibit an apparent stacked three-dimensional network (as highlighted by the blue box). In contrast, near the wood cell-wall region, the surface appears noticeably rougher and more uneven than that of WDC, suggesting the presence of a thin SiBCN ceramic-aerogel particle layer, which likely serves as the basal layer of the 3D network (as indicated by the yellow box). This layer shows no obvious interfacial gaps with the WDC substrate. A similar feature is also observed from the parallel-direction view of the wood sidewall in Figure **S1**. Therefore, we preliminarily consider it plausible that interfacial bonding may exist between WDC and the SiBCN aerogel. These structural transitions collectively validate effective SiBCN immobilization on WDC substrates.

3.2. Microwave Absorption Properties of WDC/SiBCN Aerogel Composites

In the field of microwave absorption, the RL value serves as the most commonly used and crucial parameter for evaluating the microwave absorption ability of materials [33]. When the RL value is less than -10 dB, it indicates that the material can efficiently absorb at least 90% of the incident microwave energy [34].

In addition, the frequency range covered by RL < -10 dB is defined as the EAB. This parameter plays a crucial role in comprehensively evaluating the microwave absorption performance of materials [35]. It is worth noting that for microwave-absorbing materials of different thicknesses, due to differences in their internal microstructure, electromagnetic parameters, etc., the corresponding EAB values usually vary [36].

The three-dimensional (3D) and two-dimensional (2D) RL curves of WDC are displayed in Figure **4a** and **4b**, respectively. It is noteworthy that WDC exhibits a RL_{min} of merely -10.38 dB at a thickness of 4.72 mm, with an EAB of only 0.32 GHz. These results unequivocally demonstrate that WDC possesses rather limited microwave absorption capability and fails to achieve efficient microwave absorption performance.

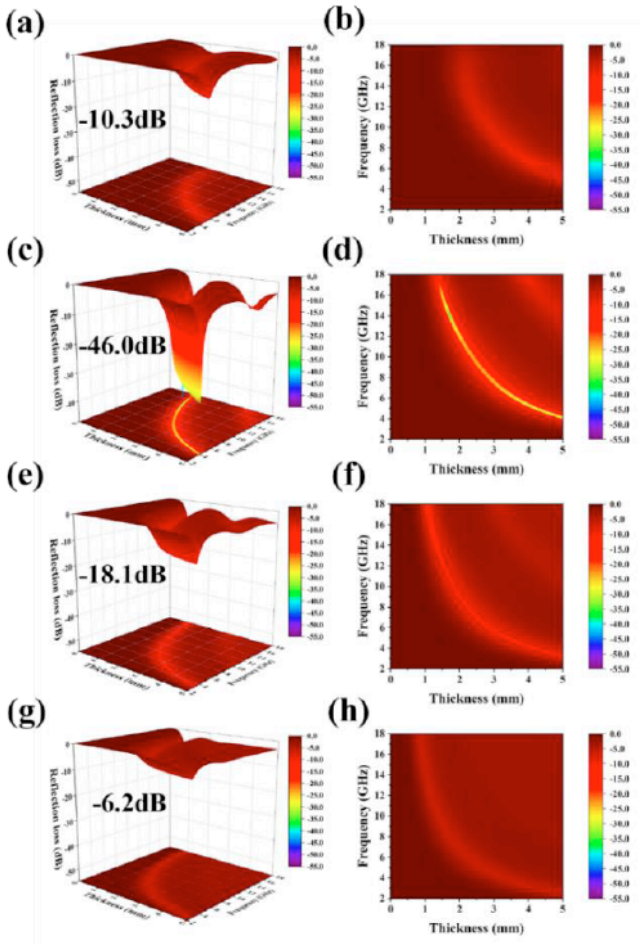

Figure 4: RL images and curves of WDC and WDC/SiBCN aerogel composites at different frequencies; (**a**, **b**) WDC; (**c**, **d**) WDC/SiBCN-5; (**e**, **f**) WDC/SiBCN-10; (**g**, **h**) WDC/SiBCN-15.

In sharp contrast, the 3D and 2D RL images of WDC/SiBCN aerogel composites with different precursor contents are shown in Figure **4c** - h. In these images, the boundary of RL = -10 dB is clearly marked with a black line. It can be found that the RL values of aerogels with different precursor contents show significant differences.

The WDC/SiBCN-5 composite exhibits the RL_{min} of -46.0 dB at a thickness of 1.71 mm, with an EAB of 3.60 GHz. In comparison, WDC/SiBCN-10 and WDC/SiBCN-15 achieve RL_{min} values of -18.1dB (EAB = 2.00 GHz) at 1.06 mm and -6.2 dB at 0.86 mm, respectively. Based on the aforementioned observations, it is evident that pristine WDC is not suitable for direct use as an absorbing material. Upon the introduction of SiBCN, the absorption performance of the samples initially increases and subsequently decreases with the increasing SiBCN content. This indicates that precise control of the SiBCN content is essential to optimize the absorption properties and

achieve a composite material with superior absorbing characteristics. Meanwhile, compared with the pure SiBCN aerogel, which exhibits a minimum reflection loss of -29 dB and an effective absorption bandwidth of 4.52 GHz (Figure **S2** (**a**) and (**b**)), WDC/SiBCN-5 shows advantage in microwave absorption performance.

To investigate the underlying mechanism of the observed phenomenon, the complex electromagnetic parameters of the composite materials were studied. Specifically, the complex permittivity ε_r ($\varepsilon_r = \varepsilon' - j\varepsilon''$) and complex permeability μ_r ($\mu_r = \mu' - j\mu''$) which play a crucial role in determining microwave absorption performance. Typically, SiBCN aerogel and carbon are considered as dielectric materials and contain no magnetic components [31]; Therefore, the influence of magnetic loss is not considered in this study [37]. Consequently, the microwave absorption capability of the composite is likely dominated by dielectric loss mechanisms (including polarization relaxation and conductive loss) rather than magnetic loss [38].

The real (ε') and imaginary (ε'') parts of the complex permittivity of the composites were systematically analyzed, which respectively characterize the electromagnetic energy storage capacity and loss characteristics of the materials [39]. As shown in Figure **5a**-**b**, with the SiBCN aerogel content increasing from 0 wt.% to 15 wt.%, the ε' values of WDC/SiBCN composites exhibited significant growth, with numerical ranges as follows: WDC (4.47-9.75), WDC/SiBCN-5 (10.28-15.75), WDC/SiBCN-10 (15.62-21.29), and WDC/SiBCN-15 (21.31-30.99). The corresponding ε'' values followed the same trend, with numerical ranges of 0.48-2.16, 2.82-5.06, 6.37-10.27, and 17.63-21.67, respectively. This phenomenon clearly demonstrates that the dielectric properties of the composites can be effectively modulated by controlling the doping concentration of SiBCN aerogel [40].

Notably, all samples exhibited typical frequency dispersion characteristics within the 2-18 GHz test band, with both the real (ε') and imaginary (ε'') parts of complex permittivity generally show an overall downward trends as frequency increased. This dielectric behavior might originates from the response characteristics of polarization relaxation mechanisms under high-frequency electromagnetic fields: when the external field frequency exceeds the characteristic frequency of the material's internal polarization relaxation, relaxation processes such as interfacial polarization and dipole orientation polarization cannot fully follow the alternating electric field variations due to response lag, leading to reduced effective permittivity [41, 42].

Figure **5c** presents the dielectric loss tangents ($tan\delta_\varepsilon = \varepsilon''/\varepsilon'$) of WDC and WDC/SiBCN composites. The $tan\delta_\varepsilon$ values of WDC range from 0.1 to 0.22, while

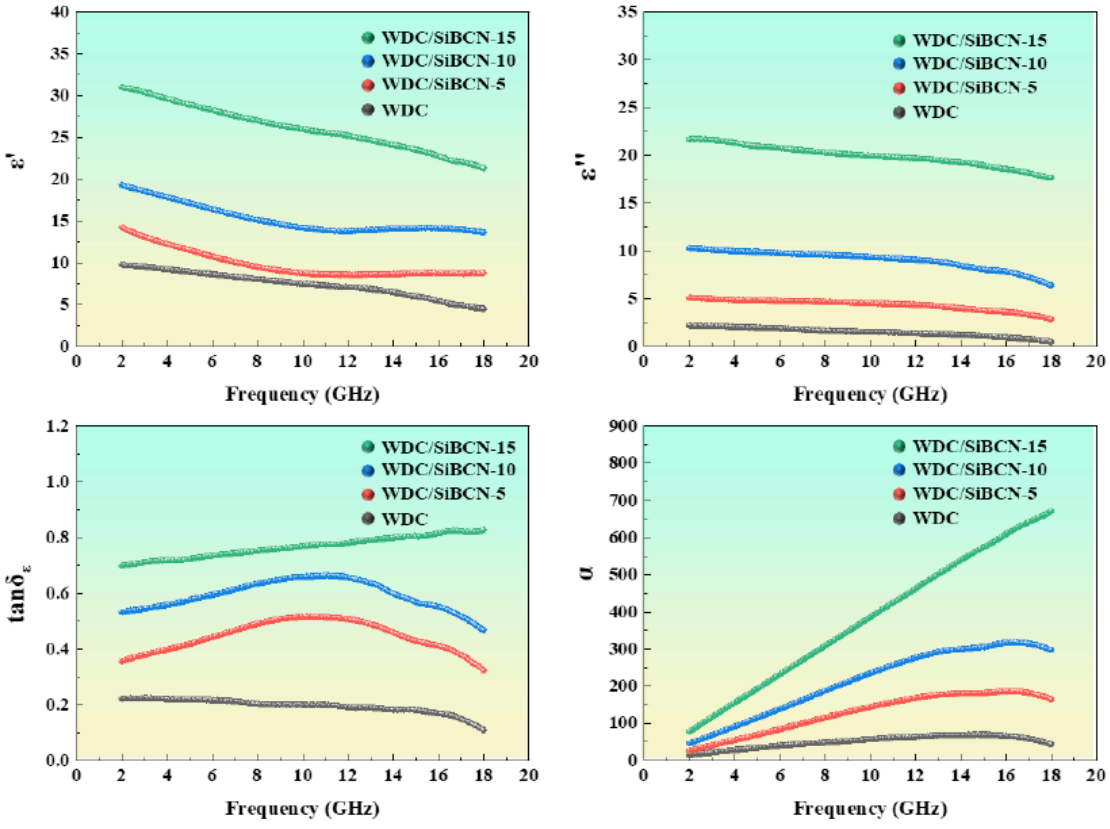

Figure 5: EM parameters and indicators of the prepared composites: (**a**) ε';(**b**) ε'';(**c**) $tan\delta_\varepsilon$; and (**d**) attenuation constant.

those of WDC/SiBCN-5, WDC/SiBCN-10, and WDC/SiBCN-15 are in the ranges of 0.27−0.44, 0.40−0.58, and 0.69−0.82, respectively. Systematic characterizations show that with the increase of SiBCN doping concentration (0−15 wt.%), the $tan\delta_{\varepsilon}$ values exhibit a significant increasing trend. This phenomenon indicates that the incorporation of SiBCN effectively enhances the dielectric loss capability of the composite system, among which the WDC/SiBCN-15 composite demonstrates the most excellent microwave energy dissipation properties, this might because the introduction of most SiBCN aerogel particles in all the samples.

To quantitatively evaluate the microwave attenuation performance of the materials, the attenuation constant (α) of the samples was calculated based on transmission line theory using Eq. (5) [43]. As a core parameter characterizing the microwave attenuation capability of the materials, the variation of this parameter directly reflects the attenuation efficiency of the composites towards incident microwaves. Figure **5d** presents the frequency-dependent attenuation constant distribution of WDC and WDC/SiBCN composites obtained through theoretical calculations. Quantitative analysis reveals a clear gradient increase in α values with increasing SiBCN content: The *α* values of WDC range from 14 to 43, those of WDC/SiBCN-5 range from 26 to 124, those of WDC/SiBCN-10 range from 45 to 317, and those of WDC/SiBCN-15 range from 77 to 671. The WDC/SiBCN-15 composite exhibits the highest α values across the entire test frequency range (2-18 GHz), while WDC shows the lowest values. This trend demonstrates excellent agreement with the previously analyzed dielectric loss tangent ($tan\delta_{\varepsilon}$) results, further confirming the superior microwave attenuation characteristics of composites with higher SiBCN content.

$$\alpha = \frac{\sqrt{2}\pi f}{c} \times \sqrt{(\mu''\varepsilon'' - \mu'\varepsilon') + \sqrt{(\mu''\varepsilon'' - \mu'\varepsilon')^2 + (\mu''\varepsilon'' + \mu'\varepsilon')^2}} \quad (3)$$

Notably, the analysis of the attenuation constant indicates that the SiBCN-15 sample exhibits the strongest dissipation capability for incident microwaves. However, this sample does not demonstrate the best overall absorption performance. This is because the absorption performance of the material is not solely determined by the attenuation constant but is also influenced by impedance matching. The impedance matching parameter reflects the amount of electromagnetic energy that can enter the material when the waves propagate to the material's surface [44, 45].

Impedance matching serves as a critical metric for evaluating the microwave coupling efficiency in microwave-absorbing materials, fundamentally reflecting the wave impedance compatibility between the material and free space. Based on transmission line theory, this property can be quantitatively characterized by the normalized impedance parameter $Z = |Z_{in}/Z_0|$ [46]. Theoretical analysis confirms that when Z near to 1, the material achieves optimal impedance matching. Particularly When $Z = 1$, the impedance of the absorbing material is completely matched with the air, and the microwave can be transmitted to the completely without being reflected [47].

As shown in Figure **6**, this study systematically investigates the impedance matching characteristics by constructing a two-dimensional thickness-frequency distribution map. The contour lines at Z =0.8 and Z =1.2 are specifically highlighted. According to microwave transmission theory [48], the region bounded by these thresholds ($0.8 \leq Z \leq 1.2$) is defined as the effective impedance matching zone [40]. Materials within this zone demonstrate efficient microwave coupling at corresponding frequency ranges and thickness parameters, providing crucial guidance for the optimized design of microwave absorbers [49].

Analysis of impedance matching characteristics (Figure **6**) reveals significant composition-dependent variations in the WDC/SiBCN aerogel composite system: The pristine WDC sample exhibits bimodal distribution within the normalized impedance matching range ($0.8 \leq Z \leq 1.2$), demonstrating two distinct high-matching regions. Notably, both WDC/SiBCN-10 and WDC/SiBCN-15 composites show constrained effective matching zones ($0.8 \leq Z \leq 1.2$), with Z-values persistently below 0.8 across the entire 2-18 GHz test spectrum, displaying characteristic broadband impedance mismatch behavior. Comparatively, WDC/SiBCN-5 demonstrates optimal impedance matching performance, which indicates that introducing more SiBCN particles is not necessarily beneficial. This composition-dependent evolution of impedance matching properties provides critical experimental evidence for establishing the structure-property relationship between SiBCN content and microwave transmission efficiency in the composite system. In addition, as shown in Figure **S2**(**c**), the impedance-matching behavior of the pure SiBCN aerogel is inferior to that of WDC/SiBCN-5. This relatively improved impedance matching of WDC/SiBCN-5 may also indirectly account for the difference in their minimum reflection loss values.

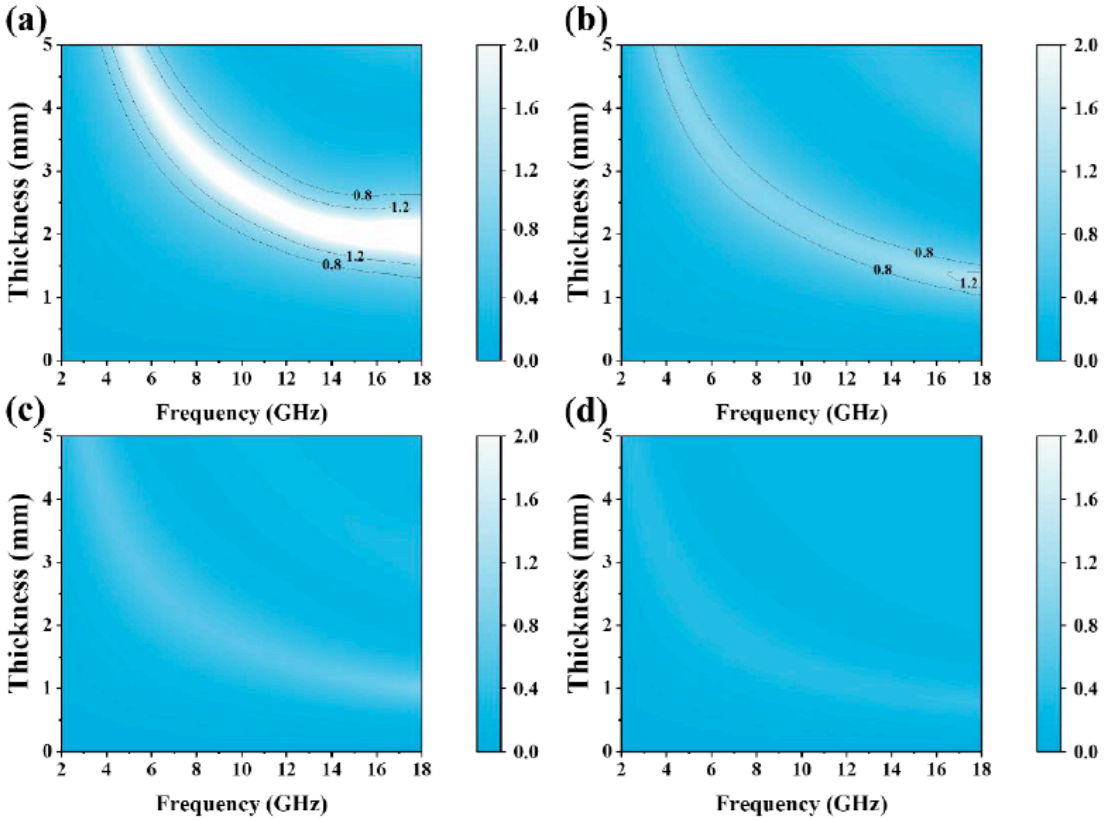

Figure 6: *Z* of the prepared composites:(**a**) WDC;(**b**) WDC/SiBCN-5;(**c**) WDC/SiBCN-10;(**d**) WDC/SiBCN-15.

Particularly noteworthy is that when the WDC/SiBCN-5 sample achieves its RL_{min} of -46.0 dB at 14.08 GHz with a matching thickness of 1.71 mm, its normalized impedance value $Z \approx 1$. Although WDC exhibits good impedance matching, its ability to attenuate microwaves is relatively weak. This is mainly due to its low α value and low $tan\delta_{\varepsilon}$ resulting in poor overall absorption performance. When the concentration of PBSZ was increased to 10% and 15%, the introduction content of SiBCN aerogel particles significantly increased, effectively enhancing its microwave attenuation capability. However, it also caused a deterioration in the overall impedance matching of the composite, thus limiting their microwave absorption performance. However, WDC/SiBCN-5 maintains good impedance matching while also possessing high attenuation capability (a larger α and $tan\delta_{\varepsilon}$ value). This means it can effectively absorb the microwave energy that enters the material. Therefore, by combining the results of impedance *Z*, attenuation coefficient α, and $tan\delta_{\varepsilon}$, WDC/SiBCN-5 demonstrates the best absorption performance, as evidenced by the RL_{min}, whereas the other materials show higher RL values due to less favorable parameters.

In addition, the wave absorption performance of WDC was compared with other similar materials, mainly including SiBCN or composites based on wood-derived carbon. Compared to the data listed in Figure **7** and Table **S1**, it can be observed that WDC/SiBCN-5 achieves better performance in RL_{min} (-46.0 dB) and EAB (3.60 GHz) than other similar materials.

The possible microwave absorption mechanisms of WDC/SiBCN aerogel composites can be divided into three parts: Firstly, dipolar polarization is possibly one of the main absorption mechanisms of this material. Under alternating electromagnetic fields, the heterogeneous interfaces between the SiBCN ceramic phase and the carbon phase generate numerous dipole moments. These dipole moments undergo continuous orientation polarization in the GHz frequency range, effectively converting electromagnetic energy into thermal energy [56]. Secondly, multiple reflection in hierarchical porous structure may also significantly contribute to the absorption performance. The hierarchical porous structure of the composite promotes extensive scattering and reflection of incident microwaves, prolonging the propagation path of microwaves within the material and creating additional phase cancellation opportunities, thereby enhancing the overall dissipation efficiency [57]. Thirdly, good impedance matching is possibly a key factor in the excellent absorption performance of the material. By integrating the effects of interfacial polarization, conductive dissipation, and structural effects, the

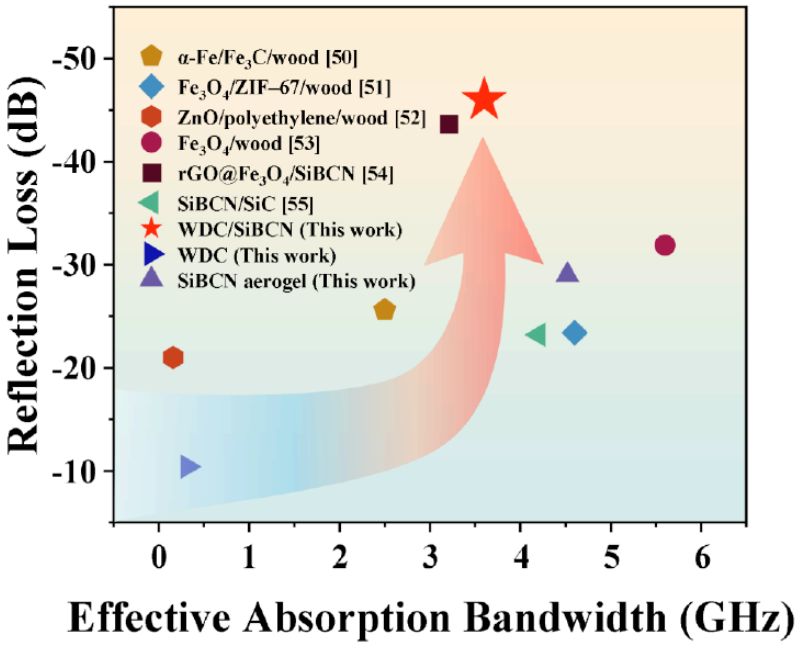

Figure 7: Comparison of microwave absorption ability for WDC/SiBCN-5 with other similar materials.

WDC/SiBCN aerogel composite achieves good impedance matching, leading to superior microwave absorption performance in the 2-18 GHz frequency range [58]. In brief, the possible mechanisms and structure–property relationship are concluded, the microwave absorption behavior can be rationalized from the structure–property relationship intrinsic to the WDC/SiBCN composite design. The rationale of constructing this hybrid lies in synergistically integrating the hierarchically porous, anisotropic wood-derived carbon scaffold with the lightweight SiBCN aerogel particulates, thereby coupling multiple dissipation pathways within a unified architecture. At a moderate SiBCN content, the aerogel particles are well dispersed on/within the porous carbon framework, which increases the density of heterogeneous interfaces and polarization centers, enhances dielectric attenuation, and simultaneously preserves an open and continuous pore network. Such a microstructure not only facilitates impedance matching by avoiding an excessively high effective permittivity, but also provides abundant internal reflection/scattering paths and an extended propagation length for incident microwaves, enabling more efficient energy dissipation. In contrast, excessive SiBCN incorporation promotes particle agglomeration and partial pore blockage, which reduces the accessible pore volume and disrupts the hierarchical transport pathways. Meanwhile, the effective permittivity tends to rise and the impedance matching deteriorates, leading to increased surface reflection and a shortened effective travel distance within the absorber; consequently, the overall absorption performance is compromised [56-58]. These possible absorption mechanisms work together to explain the exceptional performance of WDC/SiBCN aerogel composites across a wide frequency band.

CONCLUSION

In this study, a novel WDC/SiBCN aerogel composite which were designed for fully exploiting the unique microstructural advantages of both materials and thereby achieve superior performance was successfully fabricated through a three-step process involving wood carbonization, sol-gel method, and thermal treatment. This work provides a composite-design strategy that integrates a hierarchically porous, anisotropic carbon scaffold with a lightweight ceramic aerogel phase, enabling deliberate tuning of composite architecture via the PBSZ concentration which might preserve an open pore network and favorable impedance matching. Systematic investigations demonstrate that the incorporation of SiBCN nanoparticles significantly enhances the electromagnetic loss capability of the composite system. Remarkably, the sample with 5wt.% SiBCN doping exhibits optimal absorption performance, achieving a RLmin of -46.0 dB at an ultra-thin matching thickness of merely 1.71 mm, with a corresponding EAB of 3.60 GHz. These good microwave absorption properties might be related to the composite architecture combining multi-scale porosity, abundant heterogeneous interfaces, and controllable network formation. Based on its excellent overall performance and sustainable raw material sources, the WDC/SiBCN composite shows certain potential for application in the development of next-generation renewable microwave absorbing materials. Finally, mechanical robustness, structural stability, and the percolation behavior are

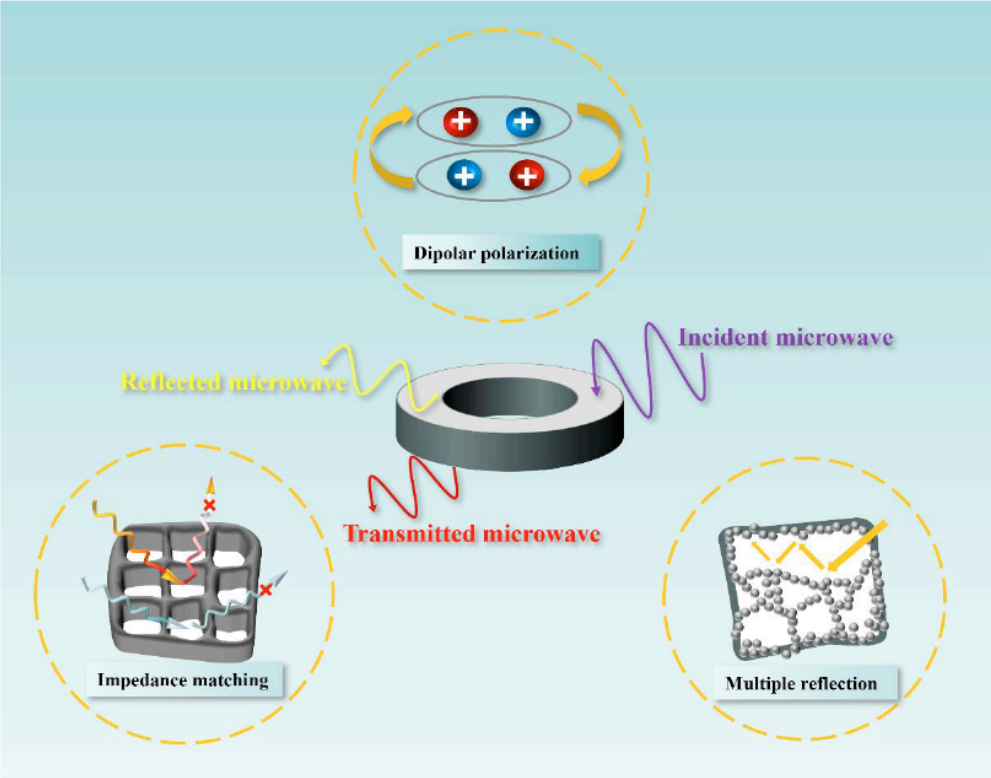

Figure 8: Microwave absorption mechanism.

also critical for practical applications and will be systematically examined in our future work."

CONFLICT OF INTEREST STATEMENT

The Authors declare that there are no relevant financial or non-financial competing interests to report.

AUTHORS' CONTRIBUTION

Yuan Ke: Writing - original draft, Formal analysis, Data curation, Conceptualization. Shangbo Han: Writing - original draft, Visualization, Methodology, Investigation. Lingyu Yang: Visualization, Investigation, Data curation. Xianqi Chen: Investigation, Formal analysis. Peitao Hu: Methodology, Visualization. Shun Dong: Supervision, Project administration, Funding acquisition. Changqing Hong: Writing – review & editing, Supervision.

ACKNOWLEDGEMENTS

The authors have no acknowledgements to declare.

FUNDING STATEMENTS

This work was supported by the National Natural Science Foundation of China (52272060, 52522203, and 52002001), Key Program of National Natural Science Foundation of China (52032003), Heilongjiang Provincial Postdoctoral Science Foundation (LBH-Z19022 and LBH-TZ2207), Heilongjiang Touyan Innovation Team Program, and Fundamental Research Funds for the Central Universities (FRFCU5710050424 and HIT-XTCX-2).

REFERENCE

[1] Wei, H., Z. Zhang, G. Hussain, L. Zhou, Q. Li, and K. (Ken) Ostrikov. Techniques to enhance magnetic permeability in microwave absorbing materials. Applied Materials Today, 2020, 19: 100596. https://doi.org/10.1016/j.apmt.2020.100596

[2] Qin, G., X. Huang, X. Yan, Y. He, Y. Liu, L. Xia, *et al*. Carbonized wood with ordered channels decorated by $NiCo_2O_4$ for lightweight and high-performance microwave absorber. Journal of Advanced Ceramics, 2022, 11(1): 105-119. https://doi.org/10.1007/s40145-021-0520-z

[3] Wu, P., J. Wang, J. Li, J. Feng, W. He, and H. Guo. Pseudo-binary composite of Sr_2TiMoO_6-Al_2O_3 as a novel microwave absorbing material. Rare Metals, 2025, 44(1): 503-514. https://doi.org/10.1007/s12598-024-03013-z

[4] Astafev, P. A., D. I. Zorin, J. A. Reizenkind, A. M. Lerer, K. P. Andryushin, A. A. Pavelko, *et al*. Microwave absorption properties of bismuth ferrite-based ceramics. Journal of Advanced Dielectrics, 2024, 14(06): 2450003. https://doi.org/10.1142/S2010135X24500036

[5] Zhou M, Gu W, Wang G, *et al*. Sustainable wood-based composites for microwave absorption and electromagnetic interference shielding[J]. Journal of Materials Chemistry A, 2020, 8(46): 24267-24283. https://doi.org/10.1039/D0TA08372K

[6] Xi, J., E. Zhou, Y. Liu, W. Gao, J. Ying, Z. Chen, *et al*. Wood-based straightway channel structure for high performance microwave absorption. Carbon, 2017, 124: 492-498. https://doi.org/10.1016/j.carbon.2017.07.088

[7] Akbar, Muh. I., B. Armynah, and D. Tahir. Comprehensive review of wood-based composites as microwave absorbers: Utilizing wood-derived materials such as carbon, metal/metal

oxides, and polymer composites as fillers. Industrial Crops and Products, 2024, 220: 119397. https://doi.org/10.1016/j.indcrop.2024.119397

[8] Hu P, Dong S, Li X, *et al*. A low-cost strategy to synthesize MnO nanorods anchored on 3D biomass-derived carbon with superior microwave absorption properties[J]. Journal of Materials Chemistry C, 2019, 7(30): 9219-9228. https://doi.org/10.1039/C9TC02182E

[9] Dong, S., W. Tang, P. Hu, X. Zhao, X. Zhang, J. Han, *et al*. Achieving excellent electromagnetic wave absorption capabilities by construction of MnO nanorods on porous carbon composites derived from natural wood via a simple route. ACS Sustainable Chemistry & Engineering, 2019, 7(13): 11795-11805. https://doi.org/10.1021/acssuschemeng.9b02100

[10] Lou, Z., C. Yuan, Y. Zhang, Y. Li, J. Cai, L. Yang, *et al*. Synthesis of porous carbon matrix with inlaid Fe_3C/Fe_3O_4 micro-particles as an effective electromagnetic wave absorber from natural wood shavings. Journal of Alloys and Compounds, 2019, 775: 800-809. https://doi.org/10.1016/j.jallcom.2018.10.213

[11] Yuan D, Chen Z, Cai C, *et al*. Microstructures, absorption and adhesion evolution of FeCoCr/silicone resin coatings at elevated temperature[J]. Frontiers in Materials, 2023, 10: 1168418. https://doi.org/10.3389/fmats.2023.1168418

[12] Zhao X, Li J, Li N, *et al*. Polymer-Derived SiOC Ceramics by Digital Light Processing-Based Additive Manufacturing[J]. Applied Sciences, 2025, 15(6): 2921. https://doi.org/10.3390/app15062921

[13] Zhang, X., L. Yang, S. Han, S. Dong, G. Chen, and J. Liu. Multifunctional mullite fiber reinforced SiBCN ceramic aerogel with excellent microwave absorption and thermal insulation performance. Ceramics International, 2024, 50(19): 35145-35153. https://doi.org/10.1016/j.ceramint.2024.06.321

[14] Tang, L., S. Chen, D. Wang, Z. Chen, J. Xue, Z. Wang, *et al*. Zirconium carbide modified SiOC composites with porous lamellar structures for broadband microwave absorption and thermal stability. Ceramics International, 2024, 50(20): 39243-39252. https://doi.org/10.1016/j.ceramint.2024.07.295

[15] Ramlow, H., L. L. Silva, C. Marangoni, M. R. Baldan, and R. A. F. Machado. Corrosion and heat-resistant SiCN/C as lightweight fibers for microwave absorption and electromagnetic field shielding in Ku-band. Diamond and Related Materials, 2024, 144: 110985. https://doi.org/10.1016/j.diamond.2024.110985

[16] Lusha, Z., T. Zicheng, R. Tusiime, W. Shaofei, F. Ningning, Z. Yifan, *et al*. Synthesis and electromagnetic wave absorbing properties of a polymer-derived SiBNC ceramic aerogel. Ceramics International, 2021, 47(13): 18984-18990. https://doi.org/10.1016/j.ceramint.2021.03.242

[17] Jiang, J., L. Yan, M. Song, Y. Li, A. Guo, H. Du, *et al*. Thermally insulated C/SiC/SiBCN composite ceramic aerogel with enhanced electromagnetic wave absorption performance. Ceramics International, 2025, 51(1): 17-24. https://doi.org/10.1016/j.ceramint.2024.10.286

[18] Song, C., Y. Liu, F. Ye, J. Wang, and L. Cheng. Microstructure and electromagnetic wave absorption property of reduced graphene oxide-SiC_{nw}/SiBCN composite ceramics. Ceramics International, 2020, 46(6): 7719-7732. https://doi.org/10.1016/j.ceramint.2019.11.275

[19] Chen, Q., D. Li, Z. Yang, D. Jia, Y. Zhou, R. Riedel, *et al*. SiBCN-reduced graphene oxide (rGO) ceramic composites derived from single-source-precursor with enhanced and tunable microwave absorption performance. Carbon, 2021, 179: 180-189. https://doi.org/10.1016/j.carbon.2021.03.057

[20] Wang, Y., C. Luo, Y. Wu, X. Hu, L. Wang, X. Chen, *et al*. High temperature stable, amorphous SiBCN microwave absorption ceramics with tunable carbon structures derived from divinylbenzene crosslinked hyperbranched polyborosilazane. Carbon, 2023, 213: 118189. https://doi.org/10.1016/j.carbon.2023.118189

[21] Sahoo, P., L. Saini, and A. Dixit. Microwave-absorbing materials for stealth application: A holistic overview. Oxford Open Materials Science, 2023, 3(1): itac012. https://doi.org/10.1093/oxfmat/itac012

[22] Zeng, X., X. Cheng, R. Yu, and G. D. Stucky. Electromagnetic microwave absorption theory and recent achievements in microwave absorbers. Carbon, 2020, 168: 606-623. https://doi.org/10.1016/j.carbon.2020.07.028

[23] Liu, J., L. Lin, J. Zhang, H. Zeng, and J. Shi. A novel process for improving the pore structure and electrochemical performance of wood-derived carbon/MnO composites. Wood Science and Technology, 2024, 58(5): 1629-1644. https://doi.org/10.1007/s00226-024-01585-8

[24] Ziherl, S., J. Bajc, and M. Čepič. Refraction and absorption of microwaves in wood. European Journal of Physics, 2013, 34(2): 449-459. https://doi.org/10.1088/0143-0807/34/2/449

[25] Gou, G., W. Hua, K. Liu, F. Cheng, and X. Xie. Bimetallic MOF@wood-derived hierarchical porous carbon composites for efficient microwave absorption. Diamond and Related Materials, 2024, 141: 110688. https://doi.org/10.1016/j.diamond.2023.110688

[26] Lv, Z., C. Lan, Y. Cao, M. Fan, Y. Ke, W. Guo, *et al*. One-step preparation of N-doped porous carbon materials with excellent microwave absorption properties based on methylene blue saturated wood-based activated carbon. Carbon Letters, 2025, 35(1): 235-244. https://doi.org/10.1007/s42823-024-00786-2

[27] Ferrari A C, Robertson J. Interpretation of Raman spectra of disordered and amorphous carbon[J]. Physical review B, 2000, 61(20): 14095. https://doi.org/10.1103/PhysRevB.61.14095

[28] Xiao, J., B. Wen, X. Liu, Y. Chen, J. Niu, S. Yang, *et al*. In-situ growth of carbon nanotubes for the modification of wood-derived biomass porous carbon to achieve efficient low/mid-frequency electromagnetic wave absorption. Journal of Colloid and Interface Science, 2024, 676: 33-44. https://doi.org/10.1016/j.jcis.2024.07.096

[29] Ba, E. C. T., M. R. Dumont, P. S. Martins, B. Da Silva Pinheiro, M. P. M. Da Cruz, and J. W. Barbosa. Deconvolution process approach in Raman spectra of DLC coating to determine the sp3 hybridization content using the ID/IG ratio in relation to the quantification determined by X-ray photoelectron spectroscopy. Diamond and Related Materials, 2022, 122: 108818. https://doi.org/10.1016/j.diamond.2021.108818

[30] Wang, H., F. Meng, F. Huang, C. Jing, Y. Li, W. Wei, *et al*. Interface modulating CNTs@PANi hybrids by controlled unzipping of the walls of CNTs to achieve tunable high-performance microwave absorption. ACS Applied Materials & Interfaces, 2019, 11(12): 12142-12153. https://doi.org/10.1021/acsami.9b01122

[31] Du, L., J. Zhang, Q. Zhou, Y. Li, Y. Zhang, X. Wang, *et al*. Hierarchical CNTs/PyC/SiBCN foam with tunable microwave absorption properties conspired by melamine-derived pyrolyzed carbon and carbon nanotubes. Carbon, 2025, 234: 120030. https://doi.org/10.1016/j.carbon.2025.120030

[32] Tai, F. C., S. C. Lee, J. Chen, C. Wei, and S. H. Chang. Multipeak fitting analysis of Raman spectra on DLCH film. Journal of Raman Spectroscopy, 2009, 40(8): 1055-1059. https://doi.org/10.1002/jrs.2234

[33] Elmahaishi, M. F., R. S. Azis, I. Ismail, and F. D. Muhammad. A review on electromagnetic microwave absorption properties: Their materials and performance. Journal of Materials Research and Technology, 2022, 20: 2188-2220. https://doi.org/10.1016/j.jmrt.2022.07.140

[34] Wang, J., M. Xia, J. Sun, H. Zhang, Q. Sun, J. Wang, *et al*. Hybrid bilayers of carbon/NiBr2 anchoring on FeSiB surface for enhanced microwave absorption coupling with smart discoloration. Rare Metals, 2025, 44(1): 489-502. https://doi.org/10.1007/s12598-024-02913-4

[35] Xu, C., X. Xiong, Y. Du, X. Lv, Z. Wu, K. Luo, *et al*. Dual-coupling networks engineering of self-assembled

ferromagnetic microspheres with enhanced interfacial polarization and magnetic interaction for microwave absorption. InfoMat, 2025, 7(4): e12645. https://doi.org/10.1002/inf2.12645

[36] Green, M., L. Tian, P. Xiang, J. Murowchick, X. Tan, and X. Chen. FeP nanoparticles: A new material for microwave absorption. Materials Chemistry Frontiers, 2018, 2(6): 1119-1125. https://doi.org/10.1039/C8QM00003D

[37] Yang, D., S. Dong, J. Xin, C. Liu, P. Hu, L. Xia, *et al*. Robust and thermostable C/SiOC composite aerogel for efficient microwave absorption, thermal insulation and flame retardancy. Chemical Engineering Journal, 2023, 469: 143851. https://doi.org/10.1016/j.cej.2023.143851

[38] Liu, J., Y. Feng, C. Liu, Y. Tong, H. Sun, H. Peng, *et al*. Novel SiBCN composite fibers with broadband and strong electromagnetic wave absorption performance. Journal of Alloys and Compounds, 2022, 912: 165190. https://doi.org/10.1016/j.jallcom.2022.165190

[39] Cheng, Z., Y. Liu, F. Ye, C. Zhang, H. Qin, J. Wang, *et al*. Microstructure and EMW absorbing properties of SiC_{nw}/SiBCN-Si_3N_4 ceramics annealed at different temperatures. Journal of the European Ceramic Society, 2020, 40(4): 1149-1158. https://doi.org/10.1016/j.jeurceramsoc.2019.11.040

[40] Zhao, M., Y. Liu, N. Chai, H. Qin, X. Liu, F. Ye, *et al*. Effect of SiBCN content on the dielectric and EMW absorbing properties of SiBCN-Si3N4 composite ceramics. Journal of the European Ceramic Society, 2018, 38(4): 1334-1340. https://doi.org/10.1016/j.jeurceramsoc.2017.10.021

[41] Li, J., Y. Hong, S. He, W. Li, H. Bai, Y. Xia, *et al*. A neutron diffraction investigation of high valent doped barium ferrite with wideband tunable microwave absorption. Journal of Advanced Ceramics, 2022, 11(2): 263-272. https://doi.org/10.1007/s40145-021-0529-3

[42] Panda, M., A. K. Thakur, and V. Srinivas. Thermal effects on the percolation behavior of polyvinylidene fluoride/nickel composites. Journal of Applied Polymer Science, 2010, 117(5): 3023-3028. https://doi.org/10.1002/app.31223

[43] Liu, M., Y. Miao, G. Wang, H. Gong, M. Sheng, J. Jing, *et al*. Polymer-derived Ni_xSi_y/graphene/SiCN composite ceramics with enhanced electromagnetic wave absorption performance. Ceramics International, 2023, 49(17): 28233-28245. https://doi.org/10.1016/j.ceramint.2023.06.078

[44] Wen, L.-C., L. Guan, J.-X. Zhang, Y.-J. Zhu, P. Chen, J.-L. Suo, *et al*. Defect engineering boosts microwave absorption in TaxNb1-xC nanowires. Rare Metals, 2025, 44(4): 2577-2588. https://doi.org/10.1007/s12598-024-03087-9

[45] Ding, C., C. Shao, Z. Wang, Z. Li, X. Guo, X. Ren, *et al*. Leaf vein micronetwork engineering enhanced energy conversion strategy for C-band ultralight yet tunable microwave absorption. Rare Metals, 2025, 44(9): 6513-6530. https://doi.org/10.1007/s12598-025-03360-5

[46] Wang, C., P. Chen, X. Li, Y. Zhu, and B. Zhu. Enhanced electromagnetic wave absorption for Y_2O_3-doped SiBCN ceramics. ACS Applied Materials & Interfaces, 2021, 13(46): 55440-55453. https://doi.org/10.1021/acsami.1c16909

[47] Huang, M., L. Wang, W. You, and R. Che. Single zinc atoms anchored on MOF-derived N-doped carbon shell cooperated with magnetic core as an ultrawideband microwave absorber. Small, 2021, 17(30): 2101416. https://doi.org/10.1002/smll.202101416

[48] Zhao, H., H. Gao, S. Jin, Y. Yao, X. Li, J. Zhang, *et al*. Exploring interfacial engineering in 3D porous, lightweight $ZnFe_2O_4$/rGO aerogel for electromagnetic wave absorption. Journal of Alloys and Compounds, 2023, 957: 170326. https://doi.org/10.1016/j.jallcom.2023.170326

[49] Liu, C., Y. Tong, C. Liu, M. Xu, H. Sun, S. Wu, *et al*. Heterogeneous interface engineering of SiBCN/Ni fibers extends enhanced electromagnetic wave absorption properties. Colloids and Surfaces A: Physicochemical and Engineering Aspects, 2024, 695: 134234. https://doi.org/10.1016/j.colsurfa.2024.134234

[50] Zhou W, Yu Y, Xiong X, *et al*. Fabrication of α-Fe/Fe_3C/woodceramic nanocomposite with its improved microwave absorption and mechanical properties[J]. Materials, 2018, 11(6): 878. https://doi.org/10.3390/ma11060878

[51] Xu L, Xiong Y, Dang B, *et al*. In-situ anchoring of Fe_3O_4/ZIF-67 dodecahedrons in highly compressible wood aerogel with excellent microwave absorption properties[J]. Materials & Design, 2019, 182: 108006. https://doi.org/10.1016/j.matdes.2019.108006

[52] Dang B, Chen Y, Shen X, *et al*. Fabrication of a nano-ZnO/polyethylene/wood-fiber composite with enhanced microwave absorption and photocatalytic activity via a facile hot-press method[J]. Materials, 2017, 10(11): 1267. https://doi.org/10.3390/ma10111267

[53] Dang B, Chen Y, Wang H, *et al*. Preparation of high mechanical performance nano-Fe_3O_4/wood fiber binderless composite boards for electromagnetic absorption via a facile and green method[J]. Nanomaterials, 2018, 8(1): 52. https://doi.org/10.3390/nano8010052

[54] C. Luo, T. Jiao, J. Gu, Y. Tang, J. Kong, Graphene shield by SiBCN ceramic: a promising high-temperature electromagnetic wave-absorbing material with oxidation resistance, ACS Appl. Mater. Interfaces 10 (45) (2018) 39307-39318. https://doi.org/10.1021/acsami.8b15365

[55] F. Ye, L. Zhang, X. Yin, Y. Zhang, L. Kong, Y. Liu, L. Cheng, Dielectric and microwave-absorption properties of SiC nanoparticle/SiBCN composite ceramics, J. Eur. Ceram. Soc. 34 (2) (2014) 205-215. https://doi.org/10.1016/j.jeurceramsoc.2013.08.005

[56] Dong, S., P. Hu, X. Li, C. Hong, X. Zhang, and J. Han. $NiCo_2S_4$ nanosheets on 3D wood-derived carbon for microwave absorption. Chemical Engineering Journal, 2020, 398: 125588. https://doi.org/10.1016/j.cej.2020.125588

[57] Cao, Q., J. Zhang, H. Zhang, J. Xu, and R. Che. Dual-surfactant templated hydrothermal synthesis of $CoSe_2$ hierarchical microclews for dielectric microwave absorption. Journal of Advanced Ceramics, 2022, 11(3): 504-514. https://doi.org/10.1007/s40145-021-0545-3

[58] Zhao, L., Q. Zhuang, G. Hu, B. Zhang, and S. Pan. Ni/porous carbon-based composite derived from poplar wood with ultrabroad band microwave absorption performance. ECS Journal of Solid State Science and Technology, 2024, 13(2): 021004. https://doi.org/10.1149/2162-8777/ad26a4

https://doi.org/10.12974/2311-8717.2025.13.14